American Mineralogist, Volume 76, pages 1547–1559, 1991

An equation of state for carbon dioxide to high pressure and temperature

Urs K. Mäder*
Department of Geological Sciences, University of British Columbia, Vancouver V6T 2B4, Canada
Robert G. Berman
Geological Survey of Canada, 601 Booth Street, Ottawa K1A 0E8, Canada

Abstract

An equation of state for fluid CO_2 is presented that yields thermodynamic properties for mineral equilibrium calculations reliably in the range 400–1800 K and 1 bar to 42 kbar with good extrapolation properties to higher pressure and temperature:

$$P = \frac{RT}{V - \left(B_1 + B_2T - \frac{B_3}{V^3 + C}\right)} - \frac{A_1}{TV^2} + \frac{A_2}{V^4}$$

with $C = B_3/(B_1 + B_2T)$ and five adjustable parameters, $B_1 = 28.06474$, $B_2 = 1.728712 \cdot 10^{-4}$, $B_3 = 8.365341 \cdot 10^4$, $A_1 = 1.094802 \cdot 10^9$, and $A_2 = 3.374749 \cdot 10^9$ in units of cm^3/mol, K, and bar.

Equation-of-state parameters were optimized simultaneously to P-V-T data up to 8 kbar and phase equilibrium data up to 42 kbar by a mathematical programming approach using the Berman (1988) data base for mineral properties. Agreement with phase equilibrium experiments is excellent. Computed volumes compare well with measurements, although they are not within uncertainties for several data sets. The enthalpy of magnesite is adjusted to −1112.505 kJ/mol to achieve consistency with phase equilibrium constraints at low pressures. New experimental brackets at 12.1 kbar (1173–1183 °C) and 21.5 kbar (1375–1435 °C) constrain the location of the equilibrium magnesite $\rightleftharpoons$ periclase + CO_2 at high pressures. Comparisons are made with existing equations of state by Kerrick and Jacobs (1981), Bottinga and Richet (1981), Saxena and Fei (1987a), and Holloway (1977).

Approximate thermophysical properties of the calcite polymorphs and aragonite were derived by mathematical programming. Results show that it is necessary to consider the high-temperature polymorphs, calcite-IV and calcite-V, to assess the validity of an equation of state for CO_2 on the basis of phase equilibrium data at high temperature.

Introduction

Volumetric properties of CO_2 at high pressures are needed for the solution of a number of problems in petrology, one of the most important being the computation of phase equilibria. Because volumes have been measured up to only 8 kbar (Shmonov and Shmulovich, 1974), extrapolation using an equation of state is required.

Equations of state for CO_2 suitable for computation of geological phase equilibria include those by Holloway (1977, 1981a, 1981b), Touret and Bottinga (1979), Bottinga and Richet (1981), Kerrick and Jacobs (1981), Powell and Holland (1985), Holland and Powell (1990), Saxena and Fei (1987a, 1987b), Shmulovich and Shmonov (1975), Mel'nik (1972), and Ryzhenko and Volkov (1971). These equations are based on a variety of theories and incorporate adjustable parameters to fit experimentally measured volumes (see Ferry and Baumgartner, 1987, and Holloway, 1987, for reviews and Prausnitz et al., 1986, for theory). Although most equations fit P-V-T data adequately, it has been pointed out that all are inconsistent with phase equilibrium data at pressures above 10–20 kbar (Fig. 1) (Haselton et al., 1978; Berman, 1988; Chernosky and Berman, 1989). Equations that use empirically combined parameters, polynomial equations in particular, may achieve excellent agreement with observed data, commonly at the expense of reasonable extrapolation. Even equations based on theory may show unconstrained behavior if they contain some empirical element. For example, Kerrick and Jacob's (1981) modified Redlich-Kwong equation (Redlich and Kwong, 1949) has no positive volume defined at progressively higher temperatures with rising pressure, because of the mathematical form of the $a(P,T)$ parameter. The equation proposed by Bottinga and Richet (1981) shows the best extrapolation properties to 42 kbar (Chernosky and Berman, 1989, and below), but it contains discontinuities that re-

---

* Present address: Geological Survey of Canada, 601 Booth Street, Ottawa K1A 0E8, Canada.

0003–004X/91/0910–1547$02.00

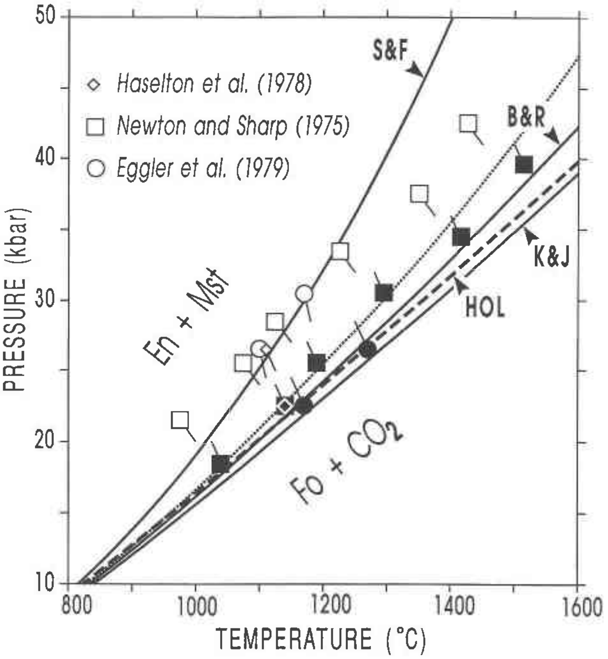

Fig. 1. Experimental brackets on the equilibrium Mst + En ⇌ Fo + CO_2 and reaction boundaries computed with the database of Berman (1988) with revised magnesite data (Chernosky and Berman, 1989; this study) and equations of state for CO_2 by Kerrick and Jacobs (1981) (K&J), Bottinga and Richet (1981) (B&R), Holloway (1977, 1981b) (dashed curve, HOL), and Saxena and Fei (1987a) (S&F). The dotted curve was computed with the B&R equation with magnesite properties perturbed by its estimated uncertainties as discussed in the text. Tails leading to the symbols depict measurement uncertainty. The diagram was produced with Ge0-Calc (Brown et al., 1988). Solid and open symbols indicate stability of Fo + CO_2 and En + Mst, respectively.

sult from separate parameter fitting for different volume intervals. Powell and Holland (1985) and Holland and Powell (1990) fitted a simple polynomial function directly to the logarithm of fugacities derived from the equation of state of Shmonov and Shmulovich (1974) and Bottinga and Richet (1981). The function is computationally efficient but limited in its applications, i.e., volumes cannot be derived reliably and extrapolation is not recommended.

To circumvent the problem of inadequate P-V-T data at high pressures, alternate approaches utilize shock wave data, although uncertainties are large. Because measurements on pure fluid CO_2 do not seem to exist, one must rely on approximations based on data for similar fluids related through corresponding state systematics (Saxena and Fei, 1987a; Helffrich and Wood, 1989). The equations chosen by these authors to fit the data are based on formulations of the intermolecular potential (e.g., Lennard-Jones). They have the disadvantage of incorporating discontinuities that require a different function for pressures below several kilobars. Saxena and Fei (1987a) fitted a modified virial equation to shock wave data valid at pressures above 5 kbar.

The purpose of the present paper is to provide petrologists with an equation of state for CO_2 that is compatible with existing experimental data, that extrapolates reliably to upper mantle conditions, and that is mathematically tractable. Preliminary results were reported by Mäder et al. (1988). A Fortran-77 coded subroutine that computes fugacity and volume at specified pressure and temperature is available from the senior author. [Requests will be answered if they are accompanied by a formatted floppy disk (IBM-compatible) and a self-addressed envelope.]

METHOD

Provided a reliable data base of thermophysical properties of minerals is available, thermodynamic properties of CO_2 may be tested by comparing calculated and experimentally determined phase equilibria (Haselton et al., 1978; Ferry and Baumgartner, 1987; Berman, 1988; Chernosky and Berman, 1989). Figure 1 indicates that existing equations of state for CO_2 calibrated on P-V-T measurements only do not extrapolate well to high pressures. An alternate approach incorporates phase equilibrium experiments as constraints rather than merely as tests of thermodynamic parameters. This is especially important in the present context because phase equilibrium data for CO_2 extend to much higher pressures (42 kbar) than P-V-T data (8 kbar).

It is important to demonstrate that the inconsistencies illustrated in Figure 1 result from inadequate equations of state for CO_2 rather than from errors in the thermodynamic properties of the minerals. This point is addressed in the section on magnesite properties below.

Mathematical programming is an appropriate tool (see Wasil et al., 1989, for a survey of computer codes) to handle this constrained optimization problem (see also Berman et al., 1986; Berman, 1988). Phase equilibrium constraints are written to separate the unknown contributions of CO_2 to the Gibbs potential from the known contributions of all other phases involved:

$$\begin{aligned}
\Delta_{R}G^{P,T} &= \sum_{i}^{\text{solids},CO_2} \nu_i \Delta_a G_i^{P,T} \\
&= \sum_{i}^{\text{solids},CO_2} \nu_i \Bigg[\Delta_f H_i^{P_r,T_r} - T\cdot S_i^{P_r,T_r} \\
&\qquad + \int_{T_r}^{T} C_{P_i}\,dT - T\cdot\int_{T_r}^{T}\left(\frac{C_{P_i}}{T}\right)dT \Bigg] \\
&\quad + \sum_{i}^{\text{solids}} \nu_i \int_{P_r}^{P} V_i^{P,T}\,dP + \nu_{CO_2}\int_{P_r}^{P} V_{CO_2}^{P,T}\,dP. \qquad (1)
\end{aligned}$$

In Equation 1 $\Delta_R G^{P,T}$ denotes the change in the Gibbs free energy of a reaction; $\Delta_a G^{P,T}$ is the apparent free energy of a pure phase as defined in Berman (1988); $\Delta_f H^{P_r,T_r}$ is the

TABLE 1. Phase equilibrium studies including pure CO_2

Reference	Equilibrium	P (kbar)	T (°C)	M	F	MB
S&A (1923)	$Cc \rightleftharpoons Lm + CO_2$	0.00–0.03	890–1210	Ga, DT	n	y
H&T (1955)	$Mst \rightleftharpoons Pe + CO_2$	0.01–2.7	650–900	CS	y	y
	$Cc \rightleftharpoons Lm + CO_2$	0.01–0.02	980–1070	CS	n	n
H&T (1956)	$Cc + \beta Qz \rightleftharpoons Wo + CO_2$	0.3–3.1	590–800	CS	n	y
G&H (1961)	$Cc \rightleftharpoons Lm + CO_2$	0.01–0.08	840–1200	GA	n	n
	$Mst \rightleftharpoons Pe + CO_2$	1.0–5.0	810–1010	GA	n	n
	$Mst \rightleftharpoons Pe + CO_2$	1.0–10	660–1090	GA	n	n
B (1962)	$Cc \rightleftharpoons Lm + CO_2$	0.00–0.03	900–1210	GA	n	y
W (1963a)	$Cc + Fo + Di \rightleftharpoons Mo + CO_2$	0.07–0.54	710–890	CS	y	y
	$Ak + Fo + Cc \rightleftharpoons Mo + CO_2$	0.5–0.7	900–930	CS	n	(y)
	$Cc + Di \rightleftharpoons Ak + CO_2$	0.08–0.7	720–930	CS	y	y
W (1963b)	$Cc + Fo \rightleftharpoons Mo + Pe + CO_2$	0.08–0.7	710–920	CS	n	n
J&M (1968)	$Mst \rightleftharpoons Pe + CO_2$	0.5–1.0	700–760	CS	y	y
J (1969)	$En + Mst \rightleftharpoons Fo + CO_2$	2.0	560	CS	y	y
S (1974)	$Cc + An \rightleftharpoons Wo + Ge + CO_2$	0.5–0.7	840–890	PC	n	(y)
	$Cc + An + Co \rightleftharpoons Ge + CO_2$	0.5–0.7	790–860	PC	y	y
I&W (1975)	$Mst \rightleftharpoons Pe + CO_2$	20–36	1350–1600	PC	y	y
N&S (1975)	$En + Mst \rightleftharpoons Fo + CO_2$	19–41	1000–1500	PC	y	y
H (1978)	$Cc + \beta Qz \rightleftharpoons Wo + CO_2$	10–19	1000–1330	PC	n	y
	$Mst + Cs \rightleftharpoons En + Fo + CO_2$	37–42	1130–1200	PC	y	y
	$En + Mst \rightleftharpoons Fo + CO_2$	24–25	1125	PC	y	y
	$Mst + Ru \rightleftharpoons Gk + CO_2$	13–37	950–1250	PC	n	i
E (1979)	$En + Mst \rightleftharpoons Fo + CO_2$	25–29	1100–1250	PC	y	y
P (1988)	$Mst \rightleftharpoons Pe + CO_2$	0.4–1.2	700–760	CS, PA	y	y
M (1990)	$Mst \rightleftharpoons Pe + CO_2$	12–21	1170–1435	PC	y	y

Note: M = experimental method; CS = cold seal, GA = gas apparatus (internally heated), PC = piston-cylinder, DT = differential thermal analysis, PA = pressure analysis. F indicates data sets used for fitting (y = yes, n = no). MB indicates consistency with Equation 5 of this study (y = yes, n = no, i = insufficient thermodynamic data on geikielite). See text for discussion of inconsistent data sets. Abbreviations of minerals: Cc = calcite, Lm = lime, Mst = magnesite, Pe = periclase, βQz = β-quartz, Fo = forsterite, Di = diopside, Mo = monticellite, An = anorthite, Co = corundum, Wo = wollastonite, Ge = gehlenite, Cs = coesite, En = orthoenstatite, Ru = rutile, Gk = geikielite. Abbreviations of authors: S&A = Smith and Adams, H&T = Harker and Tuttle, G&H = Goldsmith and Heard, B = Baker, W = Walter, J&M = Johannes and Metz, J = Johannes, S = Shmulovich, I&W = Irving and Wyllie, N&S = Newton and Sharp, H = Haselton et al., E = Eggler et al., P = Philipp, M = Mäder (1990 and this study).

enthalpy of formation from the elements; S^{P_r,T_r} is the third law entropy, and V^{P_r,T_r} is the molar volume at standard pressure (P_r = 1 bar) and temperature (T_r = 298.15 K). C_P and ν refer to the heat capacity at constant pressure and the stoichiometric coefficient, respectively. Given a reliable, internally consistent thermodynamic database for minerals, the only unknown part of Equation 1 is the last term, $\int V^{P,T}_{CO_2}\,dP$. From the relationship $\Delta_R G^{P,T} = 0$ at equilibrium, it follows that each experimental half bracket leads to an inequality of the form $\Delta_R G^{P,T} < 0$ or $\Delta_R G^{P,T} > 0$ depending on whether products or reactants are stable. Equation 1 is rearranged accordingly to impose an inequality constraint on $\int V^{P,T}_{CO_2}\,dP$ for each half bracket:

$$\nu_{CO_2}\int_{P_r}^{P} V^{P,T}_{CO_2}\,dP \lessgtr -\Delta_R G^{P,T}_{known} \tag{2}$$

where $\Delta_R G_{known}$ denotes all the terms of Equation 1 but the last one, and the "less than" refers to the case where products are stable. The f_{CO_2} is related to the volume integral by the relationship

$$RT\ln f^{P,T}_{CO_2} = \int_{P_r}^{P} V^{P,T}_{CO_2}\,dP \tag{3}$$

choosing P_r = 1 bar and assuming approximate equality of unit pressure and unit fugacity at 1 bar. R denotes the gas constant. Each inequality constraint of the form of Equation 2 requires integration of the equation of state and is therefore nonlinear with respect to parameters of the equation of state.

For this study, the internally consistent thermodynamic database of Berman (1988), including compressibility and expansivity terms, is used to compute $\Delta_R G^{P,T}_{known}$ for about 120 phase-equilibrium half brackets (Table 1). Adjustments were made to the thermodynamic properties of magnesite and calcite (see below). About 440 measured volumes were used to optimize agreement between computed and observed volumes (Table 2). The nonlinear optimization problem is solved with a general reduced-gradient strategy (GRG2, Lasden and Waren, 1982). Stability problems do not occur if the mathematical form of the equation of state is chosen carefully.

EQUATION OF STATE

There are essentially four types of equations of state from which to choose: (1) van der Waals type (Redlich and Kwong, 1949; Holloway, 1977; Touret and Bottinga, 1979; Bottinga and Richet, 1981; Kerrick and Jacobs, 1981), (2) virial type (Saxena and Fei, 1987a, 1987b), (3) molecular potential formulations (Helffrich and Wood, 1989), and (4) empirical functions to fit directly the logarithm of the fugacity (Powell and Holland, 1985; Holland and Powell, 1990). A van der Waals type of equation was chosen for the following reasons: simple mathematical form, favorable behavior in the limits ($P \rightarrow \infty$, $P \rightarrow 0$), potentially small number of adjustable parameters, and the simplest imitation of subcritical behavior. Juza (1961) presented a successfully modified van der Waals equation for H_2O applicable to pressures up to 100 kbar.

Table 2. Experimentally measured P-V-T properties of CO_2

Reference	F	T (°C)	P (kbar)	No.	Average percent deviation M&B	 PVT	 K&J	 B&R
Shmonov and Shmulovich (1974)	y	400–700	1.0–8.0	56	2.07	1.62	0.89	1.11
Tsiklis et al. (1971)	y	100–400	2.0–7.0	44	0.95	0.80	0.68	1.42
Juza et al. (1965)	y	150–475	0.7–4.0	40	1.17	0.69	0.95	0.86
Michels et al. (1935)	y	125–150	0.07–3.1	46	2.14	1.33	—	1.14
Kennedy (1954)	y	200–1000	0.03–1.4	72	0.79	0.55	1.17	0.47
Amagat (1891)	y	137–258	0.05–1.0	60	2.20	1.77	—	0.87
Vukalovich et al. (1962)	y	200–750	0.01–0.6	104	0.68	0.61	0.39	0.44
Vukalovich et al. (1963a)	n	125–150	0.02–0.6	43	1.54	1.24	—	0.83
Vukalovich et al. (1963b)	n	650–800	0.02–0.2	22	0.10	0.08	0.24	0.23
Michels and Michels (1935)	n	100–150	0.03–0.07	35	0.58	0.66	1.33	0.24

Note: Average percent deviations of calculated volumes from measured volumes are quoted for several equations of state: M&B = Equation 5 of this study, PVT = Equation 5 with parameters based on P-V-T data only (see text); K&J = Kerrick and Jacobs (1981), B&R = Bottinga and Richet (1981). F indicates data sets that were used to constrain Equation 5 (y) and data that were used for comparison only (n). No. indicates the number of data points.

An equation discussed but not adopted by Bottinga and Richet (1981) served as a starting point for our development:

$$P = \frac{\mathrm{R}T}{V - b} - \frac{A_1}{TV^2} + \frac{A_2}{V^4} \qquad (4)$$

where b, A_1, and A_2 are adjustable parameters, and R is the gas constant. The last term of Equation 4 becomes important at small volumes because of increased compressibility at high pressures. The b parameter, a measure of the "incompressible volume," is commonly assumed to be a constant, an approximation valid up to 50 kbar according to Holloway (1987). Corresponding states theory applied to the van der Waals equation predicts a b parameter of 43 cm³/mol. De Santis et al. (1974) derived a value for b of 29.7 cm³/mol for their modified Redlich-Kwong equation based on P-V-T data up to 1400 bar; the same value was adopted by Holloway (1977). The smallest measured volume is 31 cm³/mol at 7.1 kbar and 100 °C (Tsiklis et al., 1971), and shock wave data (Zubarev and Telegin, 1962) on solid CO_2 indicate a volume of 18 cm³/mol (with large uncertainties) at 180 kbar and 900 °C (as revised by Ross and Ree, 1980). It seems obvious that an equation successful at high pressures requires a compressible "incompressible volume," which may be achieved mathematically by making b dependent on volume (see also Kerrick and Jacobs, 1981; Bottinga and Richet, 1981). An inverse power of the volume dependency of the b-term was determined empirically subject to the restriction of obtaining an integrable equation. A small temperature dependence of b also proved to be advantageous, resulting in the final equation:

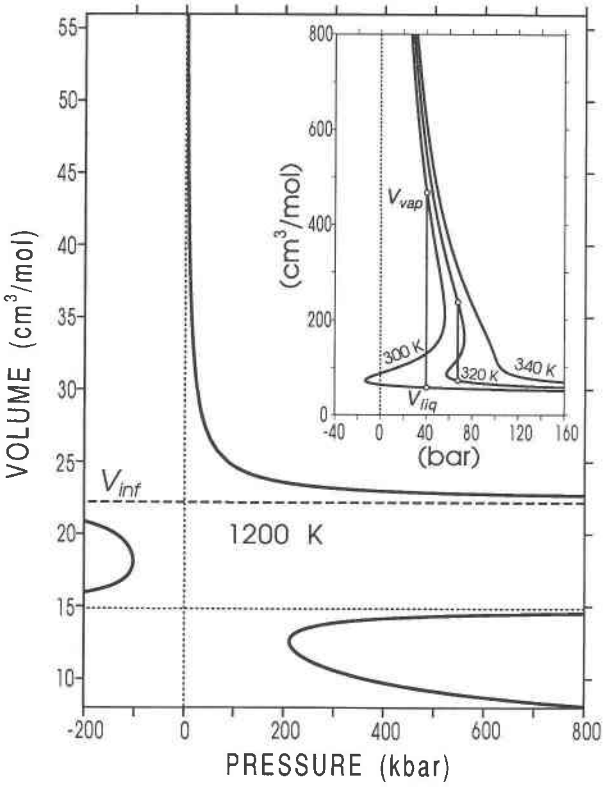

Fig. 2. Mathematical behavior of Equation 5 at 1200 K. The volume at infinite pressure is labeled V_{inf}. Inset figure depicts van der Waals behavior near the critical point with volumes of the liquid, V_{liq}, and the vapor, V_{vap}, connected by tie lines.

$$P = \frac{\mathrm{R}T}{V - \left(B_1 + B_2T - \dfrac{B_3}{V^3 + C}\right)} - \frac{A_1}{TV^2} + \frac{A_2}{V^4} \qquad (5)$$

with $C = B_3/(B_1 + B_2T)$ and five independently adjustable parameters: B_1, B_2, B_3, A_1, A_2. The A_1/TV^2 term yielded a better fit to the data than the Redlich-Kwong term $a/\sqrt{T}V(V + b)$. The function approximates the ideal gas law at very low pressures, and at infinite pressure it has a limiting volume that is dependent on temperature and parameter values (Fig. 2). The volume at specified pressure and temperature is determined iteratively, and the integration $\int V\,\mathrm{d}P$ may be performed analytically (Appendix 1). At subcritical pressures and temperatures, Equation 5 behaves like the van der Waals equation (Fig. 2, inset). The equation is continuous between 0 bar and

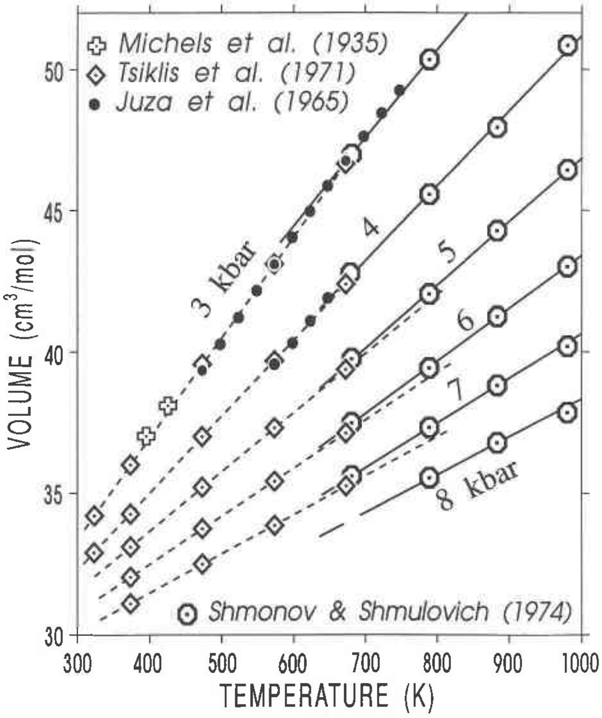

Fig. 3. Isobaric volume-temperature diagram of high-pressure P-V-T measurements. Linear trends within data sets of Shmonov and Shmulovich (solid lines) and Tsiklis et al. (dashed lines) are delineated for clarity. See text for discussion.

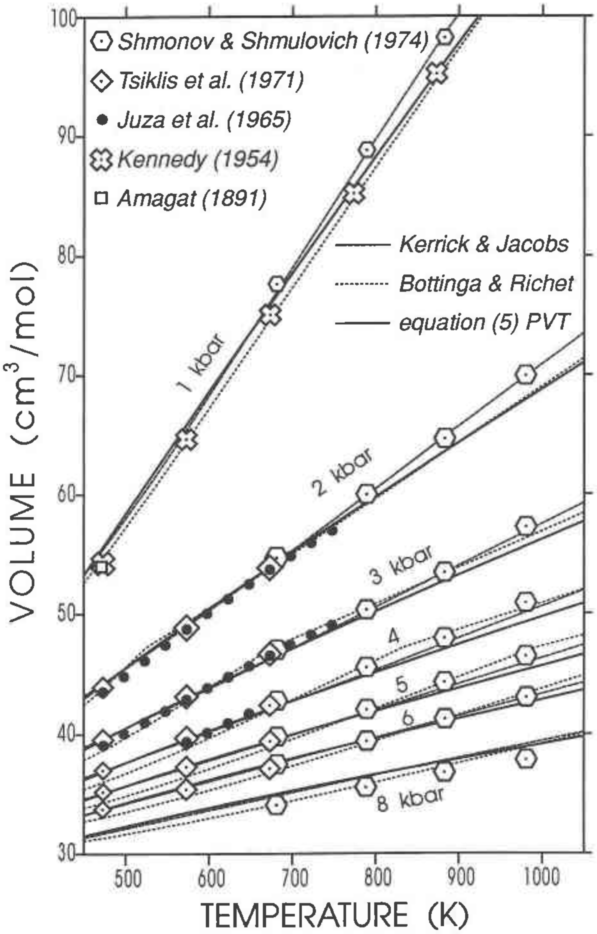

Fig. 4. Isobaric volume-temperature diagram showing comparison of different equations of state and experimentally measured volumes. Equation 5 in this figure is constrained by P-V-T data only. The discontinuities in the slopes at 47.22 cm³/mol of the Bottinga and Richet equation are a result of using separate fit parameters for different volume intervals.

infinite pressure and at temperatures above 0 K for volumes larger than the discontinuity at V_{inf} in Figure 2.

P-V-T DATA

Experimentally measured volumes (Table 2) were used to minimize the difference between computed and measured volumes during optimization. The accuracy of the P-V-T data is almost impossible to establish. Precision at pressures below 1 kbar is generally better than 0.2%, and at higher pressures it is about 0.5% depending on the type of equipment used. A complete review of equipment and quality of data through 1972 is provided by Angus et al. (1973). At lower pressures and high temperatures problems may arise from the presence of species other than CO_2 such as CO, O_2, from the precipitation of graphite, or from oxidation of the pressure vessel walls. Graphite coatings were reported by Vukalovich et al. (1963b) at temperatures above 800 °C. High-pressure equipment is prone to uncertainties because of sealing problems, calibration, thermal gradients, pressure and temperature measurement, and deformation under pressure. The nonexistent or small areas of overlap between individual high-pressure data sets make the detection of inconsistencies difficult. If, however, one extrapolates measurements from one data set into an adjacent one by some conservative method such as isobaric sections, inconsistencies of the order of 2% or more are common (Fig. 3). One of the most disturbing discrepancies is found between the 1-kbar data of Shmonov and Shmulovich (1974) and those of Kennedy (1954) (Fig. 4). This suggests that parts of entire data sets are systematically in error by more than 2%.

PHASE EQUILIBRIUM DATA

About 120 phase equilibrium experiments from 25 data sets of 16 laboratory studies (Table 1) were used to put bounds on $\int V_{CO_2}\, dP$ according to Equation 2. All phase equilibria used include magnesite or calcite as CO_2-bearing phases and only stoichiometric phases. High-pressure data sets (>25 kbar) involve magnesite only. Studies including dolomite were avoided because of uncertainties stemming from its ordering state (see also Berman, 1988). Similarly, phase equilibria including geikielite, meionite, spurrite, and tilleyite were not considered. A thermodynamic analysis of the system CaO-SiO_2-CO_2 at high temperatures is provided by Treiman and Essene (1983) including larnite, rankinite, spurrite, and tilleyite. Reactions

TABLE 3. Constraints on f_{CO_2} imposed by experimental brackets on the equilibrium Mst + En ⇌ Fo + CO_2 (Newton and Sharp, 1975)

	P	*T*	*P*	*T*	$RT \ln f_{CO_2}$					
St.	Exp. (kbar)	Exp. (K)	Adj. (kbar)	Adj. (K)	Obs. (kJ)	M&B (kJ)	B&R (kJ)	K&J (kJ)	S&F (kJ)	Hol (kJ)
Re	19.0	1273	20.5	1248	>154.6	158.9	161.7	163.2	156.6	162.5
Pr	19.0	1298	17.5	1313	<158.2	154.7	157.8	**159.0**	153.3	157.4
Re	32.0	1523	33.5	1498	>213.6	220.6	224.6	227.6	**213.0**	228.3
Pr	32.0	1553	30.5	1568	<219.4	217.9	**222.4**	**225.1**	211.2	**224.3**
Re	41.0	1723	42.5	1698	>260.0	265.2	270.1	274.4	**253.0**	275.9
Pr	41.0	1773	39.5	1788	<268.9	264.7	**270.4**	**274.3**	253.2	**274.0**

Note: St. indicates whether reactants (Re) or products (Pr) are stable. Adj. shows pressures and temperatures adjusted for experimental uncertainties. Obs. (observed) was computed with Equation 2 and the data base of Berman (1988) with revised magnesite properties (see text). The remainder of the columns were computed with various equations of state: M&B = Equation 5 of this study, B&R = Bottinga and Richet (1981), K&J = Kerrick and Jacobs (1981), S&F = Saxena and Fei (1987a), Hol = Holloway (1977). Numbers printed in bold face are inconsistent with experimental brackets (Obs.).

including calcite were only used below the transition of calcite-I to calcite-IV (ca. 790 °C) because of poorly constrained properties of calcite-IV and calcite-V (see section below). The equilibrium En + Mst ⇌ Fo + CO_2, constrained between 19 and 41 kbar by three studies (Newton and Sharp, 1975; Haselton et al., 1978; Eggler et al., 1979), forms one of the cornerstones of the present work. Equally important are tight constraints on the equilibrium magnesite ⇌ periclase + CO_2 at low pressures (Philipp, 1988) and at high pressures (new experiments, this study).

Experimental uncertainties were accounted for by displacing positions of the half brackets away from the equilibrium based on best estimates of uncertainties in pressure and temperature. Table 3 shows an example of how one data set (Newton and Sharp, 1975) is treated to impose constraints on the CO_2 between 19 and 41 kbar and 1373 and 1773 K. Many of the experimental studies used as constraints in this paper do not properly demonstrate reversibility of the phase equilibria studied. This is accounted for by increasing the range of uncertainty on the side of the equilibrium boundary approximated by stability or synthesis experiments rather than reversals. This is in most cases the reactant-stable side.

NEW EXPERIMENTS ON MAGNESITE ⇌ PERICLASE + CO_2

Existing experiments by Irving and Wyllie (1975) on the equilibrium magnesite ⇌ periclase + CO_2 do not constrain the equilibrium position at high pressure. The equilibrium was therefore reversed at 12.1 kbar between 1173 and 1183 °C and at 21.5 kbar between 1375 and 1435 °C in a piston-cylinder apparatus using ¾-in. talc-pyrex assemblies. Friction corrections were calibrated against the melting curve of Au and Ag (Mirwald et al., 1975); they amounted to 2.9 kbar at 15 kbar and 3.5 kbar at 25 kbar nominal pressure. Thermal gradients and the effect of pressure on the electromotive force of the Pt-Pt10%Rh thermocouples (Getting and Kennedy, 1970) were accounted for. Uncertainties are estimated at ±1.0 kbar and ±10 K. Details are reported elsewhere (Mäder, 1990, and in preparation).

MAGNESITE PROPERTIES

The standard state properties, $\Delta_f H^{P_r,T_r}$, S^{P_r,T_r}, and V^{P_r,T_r}, of all minerals involved in the equilibria of Table 1 are tightly constrained by calorimetry and low-pressure phase equilibrium data (see Berman, 1988, for details). The most poorly constrained properties are those for magnesite, particularly the heat capacity and thermal expansivity, for which the data extend only to 750 K (Kelly, 1960) and 773 K (Markgraf and Reeder, 1985), respectively. The sensitivity of the calculated phase equilibria to possible errors in extrapolation of these magnesite properties can be examined by adjusting the functions given by Berman (1988) and Chernosky and Berman (1989) within experimental uncertainties so that the inconsistencies between existing equations of state and phase equilibrium data are minimized. The heat capacity function of Berman (1988), adjusted from Berman and Brown (1985), is already aimed at minimizing inconsistencies with the Kerrick and Jacobs (1981) equation of state at high pressure, i.e., to render magnesite less stable. To decrease the stability of magnesite, the thermal expansion was maximized while maintaining average percent deviations from measured values within 100% of those computed with the best fit of Berman (1988). This results in an increase of 25% of the v_4 term and a decrease of 21% of the v_3 term (to adjust for increased curvature) compared to Berman (1988) using his Equation 5, $V^{P,T}/V^{P,T_r} = 1 + v_3(T - T_r) + v_4(T - T_r)^2$. Phase equilibria computed with this perturbed volume function for magnesite are still inconsistent with all equations of state for CO_2 (Fig. 1). It is concluded that inconsistencies cannot be attributed entirely to errors in the properties of minerals and that, instead, phase equilibrium data may be used to constrain the high-pressure properties of CO_2.

At pressures below 10 kbar and temperatures below 800 °C, magnesite properties are well constrained and any consistent set analysis (e.g., Berman, 1988) is not hampered by uncertainties in CO_2 properties because existing equations of state do not differ significantly at pressures below 10 kbar. It is therefore possible to derive standard state thermodynamic properties of magnesite prior to the optimization of CO_2 properties at higher pressures. Cher-

TABLE 4. Thermodynamic properties of calcite polymorphs and magnesite

Std. state prop.	$\Delta_f H^{P_r,T_r}$ (kJ/mol)	S^{P_r,T_r} (J/mol·K)	V^{P_r,T_r} (J/bar)		Reference
Aragonite	−1207.597	87.490	3.415		(*), (*), (1)
Calcite(-I)	−1206.970	91.893	3.690		(*), (*), (B)
Calcite-IV	−1204.580	94.100	3.683		(*), (*), (*)
Calcite-V	−1199.768	97.895	3.689		(*), (*), (*)
Magnesite	−1112.505	65.090	2.803		(*), (B), (B)
C_P coefficients	k_0	k_1 ($\times 10^{-2}$)	k_2 ($\times 10^{-5}$)	k_3 ($\times 10^{-7}$)	
Calcite(-I)	178.19	−16.577	−4.827	16.660	(2, 3, 4, B)
Ar, Cc-IV, Cc-V	178.19	−16.577	−4.827	16.660	(a)
Magnesite	194.08	−21.210	−1.533	17.491	(BB)
V coefficients	v_1 ($\times 10^{6}$)	v_2 ($\times 10^{12}$)	v_3 ($\times 10^{5}$)	v_4 ($\times 10^{10}$)	
Aragonite	−1.620	0.0080	3.670	227.4	(5, 6, 7), (5, 8)
Calcite(-I)	−1.400	0.0060	0.8907	227.4	(B), (a), (B), (B)
Cc-IV, Cc-V	−1.400	0.0060	0.8907	227.4	(a)
Magnesite	−0.890	0.0221	1.844	416.0	(CB), (B)

Note: Standard state thermodynamic properties of calcite polymorphs at 1 bar and 298.15 K, isobaric heat capacity function coefficients (k_0–k_3), and volume function coefficients (v_1–v_4). The heat capacity function of Berman and Brown (1985) is used: $C_P = k_0 + k_1 T^{-0.5} + k_2 T^{-2} + k_3 T^{-3}$; the volume function of Berman (1988) is used: $V^{P,T}/V^{P_r,T_r} = 1 + v_1(P - P_r) + v_2(P - P_r)^2 + v_3(T - T_r) + v_4(T - T_r)^2$. C_P is in J/mol·K and V in J/bar, T in K, P in bar. References: B = Berman (1988), BB = Berman and Brown (1985), CB = Chernosky and Berman (1989), * = values derived in this study, a = assumed, see text for discussion, 1 = Robie et al. 1979, 2 = Stavely and Linford (1969), 3 = Jacobs et al. (1981), 4 = Kelly (1960), 5 = Salje and Viswanathan (1976), 6 = Madelung and Fuchs (1921), 7 = Singh and Kennedy (1974), 8 = Kozu and Kani (1934).

nosky and Berman (1989) revised the enthalpy of formation for magnesite (−1114.505 kJ/mol) based on experimental constraints on phase equilibria in systems with an H_2O-CO_2 fluid phase. Trommsdorff and Connolly (1990) propose an increase of the Gibbs free energy of formation for magnesite (an enthalpy of about −1111 kJ/mol) based on field evidence of phase diagram topologies (CaO-MgO-SiO_2-CO_2-H_2O) and new phase equilibrium experiments by Philipp (1988) on the equilibrium magnesite ⇌ periclase + CO_2.

A value of −1112.505 kJ/mol for the enthalpy of formation from the elements for magnesite was derived in this study by linear programming analysis. This value is consistent with Philipp's (1988) accurate pressure analysis experiments and with the brackets on the same equilibrium determined by Harker and Tuttle (1955) and Johannes and Metz (1968) using conventional cold-seal techniques. This value used in conjunction with the data base of Berman (1988) produces the essential features of the phase diagram topologies suggested from natural mineral assemblages as outlined by Trommsdorff and Connolly (1990). The destabilization of magnesite was minimized in order not to deviate more than necessary from experimental constraints in systems including magnesite and an H_2O-CO_2 fluid mixture (e.g., magnesite + talc ⇌ forsterite + H_2O + CO_2, Greenwood, 1967). Any such discrepancy has to be counterbalanced by more nonideal mixing of H_2O-CO_2 (larger excess volume on mixing) compared with the mixing model of Kerrick and Jacobs (1981) if all other thermodynamic parameters are well constrained.

The uncertainty on extrapolating heat capacity and thermal expansion of magnesite is the largest single contribution to the uncertainty of the CO_2 properties derived in this study. The preferred thermophysical properties of magnesite are summarized in Table 4.

RESULTS

The ability of Equation 5 to fit P-V-T data in the absence of additional constraints from phase equilibrium experiments is demonstrated in Figure 4. The following equation-of-state parameters are derived: $B_1 = 29.5713$, $B_2 = 3.16418 \cdot 10^{-4}$, $B_3 = 10.2554 \cdot 10^{4}$, $A_1 = 1.10002 \cdot 10^{9}$, $A_2 = 2.54456 \cdot 10^{9}$, in units of cm^3/mol, K, and bar. The results are difficult to compare with other equations of state because each was calibrated with different weights given to various sets of data. Figure 4 shows only the high-pressure subset of all constraining P-V-T measurements, with the overall quality of fit of the three equations being comparable (Table 2). The equations share one feature: volumes extrapolated toward high pressures are larger than those inferred from the high-pressure P-V-T data of Shmonov and Shmulovich (1974).

Phase equilibrium constraints at pressures below 8 kbar are fully compatible with P-V-T data and the equation of state. The high-pressure phase equilibrium constraints (Table 1), however, are not compatible. The prominent feature observed is, as would be expected from Figures 1 and 4, that the $RT \ln f_{CO_2}$ terms and thus the volumes are forced to become smaller (more stable CO_2) compared with predictions based on P-V-T data alone (Fig. 5). The final equation-of-state parameters, incorporating phase equilibrium constraints, are given in Table 5. Table 3 lists the magnitudes of mismatch for several equations of state compared with experimental data by Newton and Sharp (1975).

Table 1 summarizes the consistency of Equation 5 with phase equilibrium experiments involving pure CO_2 and

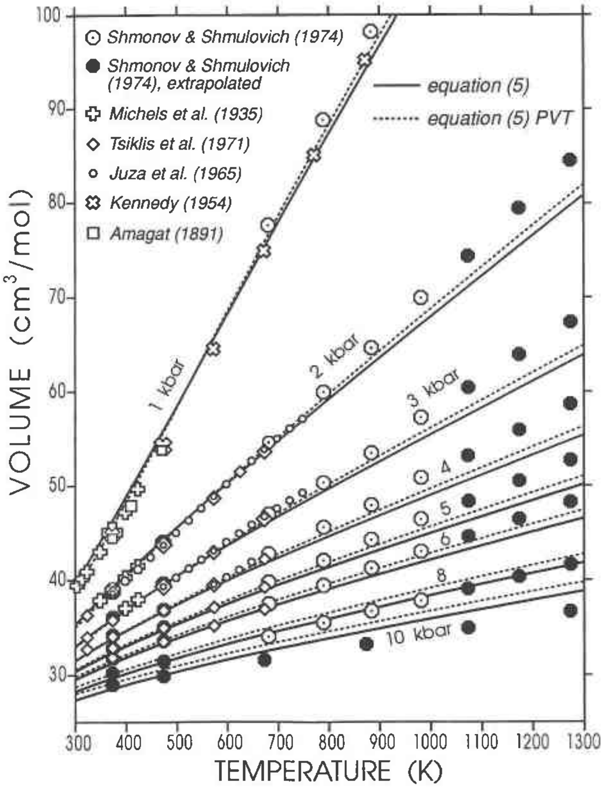

Fig. 5. Isobaric volume-temperature diagram comparing Equation 5 constrained by P-V-T measurements only (dashed lines) with Equation 5 constrained additionally by phase equilibrium experiments (solid lines). Filled hexagons depict volumes extrapolated by Shmonov and Shmulovich based on their own experimental data (hexagons with dots). The 9-kbar and 7-kbar data points and curves are omitted for clarity.

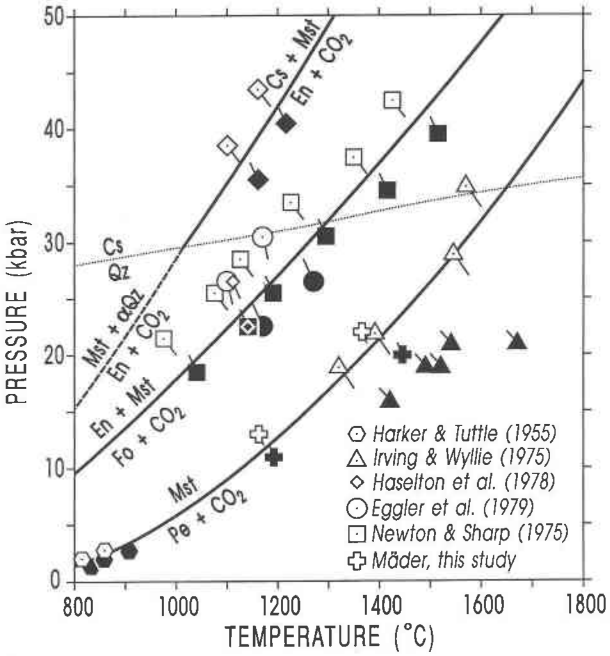

Fig. 6. Pressure-temperature diagram with phase equilibria involving magnesite computed with the equation of state for CO_2 of this study compared with phase equilibrium experiments. A friction correction of −3 kbar was applied to the brackets by Irving and Wyllie (1975) based on calibrations by Huang and Wyllie (1975). Abbreviations of minerals: Cs = coesite, Mst = magnesite, En = orthoenstatite, Fo = forsterite, Pe = periclase, Qz = quartz. Tails leading to symbols depict measurement uncertainties. The diagram was produced with Ge0-Calc (Brown et al., 1988). Solid and open symbols indicate stability of En + CO_2 and Mst + SiO_2, respectively.

stoichiometric phases. The two data sets that are inconsistent with the equation include some experiments by Goldsmith and Heard (1961) with P_{CO_2} likely less than P_{tot} and one set by Walter (1963b) that is inconsistent (>100 K) with any other data. Berman (1988) attributes the latter inconsistency to Walter's failure to recognize periclase in any experimental products. Figure 6 compares computed high-pressure phase equilibria including magnesite with experimental data. Reactions, including high-temperature polymorphs of calcite, calcite-IV, and calcite-V, are discussed in a separate section below. The equation of state thus performs reliably up to at least 42 kbar.

Figure 5 and Table 2 document the comparison of measured and calculated volumes. Agreement at low pressures and supercritical temperatures is excellent because the equation approximates the ideal gas law. The equation was not constrained by data below 373 K, and therefore the shape of the subcritical area is only approximate and solely a result of its van der Waals mathematical form. Between 100 °C and −10 °C the volumes of the fluid, liquid, or vapor deviate not more than 0.5% from measurements except very close to the critical point. At −50 °C (5–300 bar), computed volumes are too small by 2.5% compared with measurements. The critical curve cannot be adequately represented with only five parameters because of the severe mathematical constraints imposed by equating f_{liquid} to f_{vapor}. The calculated critical point is at 332.74 (± 0.01) K, 88.754 (± 0.001) bar, and 115.3 (± 0.3) cm³/mol. Experimentally determined values (Angus et al., 1973) are 304.20 (± 0.05) K, 73.858 (± 0.05) bar, and 94.07 (± 0.1) cm³/mol.

Table 5. Parameter values for Equation 5

B_1	B_2	B_3	A_1	A_2
28.0647	$1.72871 \cdot 10^{-4}$	$8.36534 \cdot 10^{4}$	$1.09480 \cdot 10^{9}$	$3.37475 \cdot 10^{9}$

Note: Units are cm³/mol, K, and bar. R = 83.147.

Rigorous comparisons of computed CO_2 properties with experimental phase equilibria have previously been hampered by insufficient thermophysical data of solid phases, magnesite in particular (Haselton et al., 1978; Bottinga and Richet, 1981). The properties of solids chosen by Saxena and Fei (1987a) lead to good agreement with CO_2 properties obtained with their equation of state and render the Bottinga and Richet (1981) equation grossly inconsistent at 40 kbar pressure. This is in contrast with our computations (cf. Fig. 1), which render CO_2 far too stable with the Saxena and Fei (1987a) equation. This discrepancy results, at least in part, from Saxena and Fei's choice of heat capacity function (Robie et al., 1979) not suitable for extrapolation beyond the highest temperature data for magnesite (750 K).

Equation 5 is able to fit measured volumes significantly better without the additional constraints from phase equilibria (Fig. 5); the notable exceptions are volumes measured at the highest pressures, which show excellent agreement. This may indicate too little flexibility of the equation, some systematic problems with high-pressure experimental P-V-T equipment, or inaccurate mineral properties used to constrain the parameters. It seems that a more complex equation is not justified with the amount, extent, and quality of P-V-T data available.

Additional volumetric constraints imposed by shock wave data could possibly improve the extrapolation properties of Equation 5 toward pressures above 100 kbar. Shock wave measurements (Zubarev and Telegin, 1962) on solid CO_2 (or more likely a mixture of solid and liquid at initial conditions) are difficult to apply, and shock measurements on liquid CO_2 appear to be nonexistent. The equation of state based on shock data of similar fluids and corresponding state systematics of Saxena and Fei (1987a) is inconsistent with phase equilibrium experiments (Table 3, Fig. 1). A new approach taken by Helffrich and Wood (1989) appears to bridge shock wave data and phase equilibrium data more successfully.

In summary, the region where our proposed equation performs reliably spans 400–1773 K and 1 bar to 42 kbar. Extrapolation to higher pressures and temperatures is expected to yield useful results, possibly to 80 kbar and 2300 K.

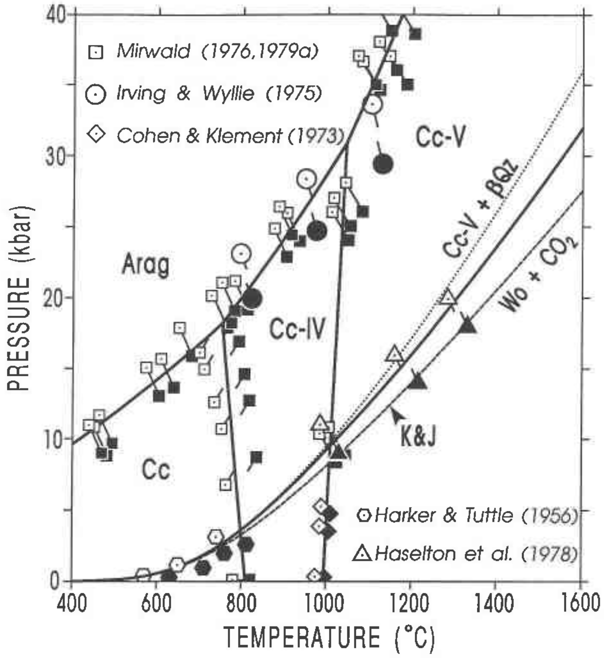

Fig. 7. Pressure-temperature diagram with phase equilibria involving calcite polymorphs computed with thermodynamic properties of Table 4 and Berman (1988) and the equation of state for CO_2 of this study. Solid symbols indicate the stability of the low-pressure, high-temperature assemblages. Open symbols indicate the stability of the high-pressure, low-temperature assemblages. The dotted curve shows the position of the wollastonite equilibrium calculated with calcite-I (omitting Cc-IV and Cc-V). The dashed curve was computed with the Kerrick and Jacobs (1981) equation of state not considering any of the high-temperature calcite polymorphs. Abbreviations of minerals: Arag = aragonite, Cc = calcite, βQz = β-quartz, Wo = wollastonite. Tails leading to symbols depict measurement uncertainties. The diagram was produced with Ge0-Calc (Brown et al., 1988).

CALCITE (I-IV-V)–ARAGONITE

In calibrating the equation of state, inconsistencies became evident between constraints on f_{CO_2} imposed by magnesite phase equilibria and those by calcite reactions. The well-constrained high-pressure brackets on En + Mst $\rightleftharpoons$ Fo + CO_2 and those on Mst $\rightleftharpoons$ Pe + CO_2 (Fig. 6) demand smaller f_{CO_2} (more stable CO_2) than high-pressure brackets on Cc + βQz $\rightleftharpoons$ Wo + CO_2 (Fig. 7). One likely explanation is the presence of the more stable calcite polymorphs calcite-IV and calcite-V (e.g., Mirwald, 1976, for nomenclature and summary) at high temperatures, which would tend to shift the above equilibrium to higher temperatures.

As a first step, all experimental brackets including calcite at high temperatures were not considered as constraints on the properties of CO_2 in order to remove the possibly significant effects of calcite-IV and calcite-V. To test the above hypothesis, thermophysical properties of the calcite polymorphs were derived from constraints imposed by the aragonite–calcite-I–calcite-IV–calcite-V phase diagram.

Unfortunately, few quantitative data are available on the unquenchable polymorphs calcite-IV and calcite-V. The transition boundaries have been the subject of numerous studies (Boeke, 1912; Eitel, 1923; Clark, 1957; Bell and England, 1964; Crawford and Fyfe, 1964; Boettcher and Wyllie, 1968; Johannes and Puhan, 1971; Crawford and Hoersch, 1972; Cohen and Klement, 1973; Irving and Wyllie, 1975; Mirwald, 1976, 1979a, 1979b). The phase transitions between calcite-I-IV-V are most likely related to order-disorder within the anion sublattice (Lander, 1949; Salje and Viswanathan, 1976; Mirwald, 1979a, 1979b; Dove and Powell, 1989). There is, however, still some debate about the existence and exact nature of discrete phase transitions in calcite (Markgraf and Reeder, 1985). To minimize the number of thermophysical parameters to be derived, all polymorphic transitions were treated as first-order phase transitions with small volume discontinuities at the phase boundaries. This should lead to a reasonable first approximation of the energetics of these phase transitions in the absence of sufficient constraints on the order-disorder processes.

In view of the lack of data on thermal and volumetric properties, the following assumptions were made: (1) All polymorphs share the same heat capacity function. Experimental data by Kobayashi (1950b) that suggest a lower heat capacity for aragonite than calcite were disregarded because his aragonite and calcite (Kobayashi, 1950a) data are imprecise and inconsistent with data of other studies (Stavely and Linford, 1969; Jacobs et al., 1981; Kelly, 1960). (2) Calcite-IV and calcite-V share the same expansivity and compressibility as calcite-I. X-ray data by Mirwald (1979a) suggest a larger thermal expansion for Cc-IV than for Cc-I, which is however not observed in Markgraf and Reeder's (1985) measurements. The extremely large thermal expansion of aragonite relative to calcite suggested by measurements up to 450 °C (Salje and Viswanathan, 1976; Kozu and Kani, 1934) was reduced by 15% during fitting in order to constrain the curvature of the Cc ⇌ Ar equilibrium to the phase equilibrium data. The difference in compressibility between calcite and aragonite was derived from studies that include measurements on both minerals by the same technique (Salje and Viswanathan, 1976; Madelung and Fuchs, 1921). All other thermodynamic properties were fitted to measurements as summarized in Table 4. Calcite-I properties are nearly identical to those in Berman (1988) and are compatible with the phase equilibrium experiments of Table 2.

The standard state properties ($\Delta_f H^{P_r,T_r}$, S^{P_r,T_r}, V^{P_r,T_r}) of Cc-IV and Cc-V were refined by mathematical programming analysis using phase equilibrium constraints (Cc-I ⇌ Ar, Cc-IV ⇌ Ar, Cc-V ⇌ Ar, Cc-I ⇌ Cc-IV, Cc-IV ⇌ Cc-V; Fig. 7). The derived thermophysical properties are consistent with most phase equilibrium studies with the exception of the Ar ⇌ Cc-I transition at low temperatures (<200 °C) and the Ar ⇌ Cc-V transition. At 100 °C, the computed Arag ⇌ Cc-I boundary is located 0.5 kbar too low compared with experiments by Crawford and Fyfe (1964). Data of Mirwald (1979a) on the Ar ⇌ Cc-V equilibrium are inconsistent and not compatible with the brackets obtained by Irving and Wyllie (1975) (Fig. 7). This boundary is therefore poorly constrained and allows some latitude in the properties of Cc-V.

Computed phase equilibria involving Cc-I, Cc-IV, and Cc-V (Fig. 7) are consistent with all phase equilibrium experiments (Table 1) with the exception of small inconsistencies (<4 K) with one half bracket on the reaction Ak + Cc-IV + Fo ⇌ Mtc + CO_2 (Walter, 1963a) and An + Cc-IV ⇌ Wo + Ge + CO_2 (Shmulovich, 1974). Most importantly, however, the computed equilibria are compatible with the high-pressure brackets on the reaction Cc-IV/V + βQz ⇌ Wo + CO_2 (Haselton et al., 1978) and the high-temperature brackets on the equilibrium Cc-(IV/V) ⇌ Lime + CO_2 (Smith and Adams, 1923; Baker, 1962). It appears that only the experimental data of Smith and Adams (1923) and Baker (1962) for the calcite decarbonation can be reconciled with the calorimetric data of lime and the above treatment. The data of Harker and Tuttle (1955) and Goldsmith and Heard (1961) are inconsistent. Smith and Adams' (1923) differential thermal analysis experiments are, however, not reversed and constrain only the product-stable assemblage.

CONCLUSIONS

The following points are emphasized: (1) phase equilibrium brackets put important constraints on the f_{CO_2} at pressures not accessible by conventional *P-V-T* measurements, (2) mathematical programming analysis of *P-V-T* and phase equilibrium data allows significant improvements of the equation of state for CO_2, and (3) some experimentally measured volumes of CO_2 at high pressures may have much larger uncertainties than previously estimated.

The data needed for further improvements include (1) more high-quality phase equilibrium brackets at high pressures on reactions involving CO_2, (2) a set of carefully measured CO_2 volumes up to 12 kbar, (3) shock wave data on fluid CO_2, (4) measurements on the expansivity of magnesite to high temperatures under pressure, and (5) quantitative evaluation of the complex phase transitions undergone by calcite. Progress is required in providing mathematically practical equations of state with a theoretical basis.

ACKNOWLEDGMENTS

The senior author is indebted to H.J. Greenwood for support and advice during U.M.'s Ph.D. thesis research. The manuscript was improved by H.J. Greenwood and T.H. Brown. Helpful reviews were provided by N. Chatterjee, M. Ghiorso, and an anonymous reviewer. J.R. Holloway kindly supplied computer codes for the evaluation of his equation of state. We gratefully acknowledge financial support by NSERC to R.G.B. (OGP 0037234) and H.J. Greenwood (U.M.) (67-4222) and funds to H.J. Greenwood (U.M.) administered by the British Columbia Ministry of Energy, Mines and Petroleum Resources under the Canada–British Columbia Mineral Development Agreement.

REFERENCES CITED

Amagat, E.M. (1891) Nouveau réseau d'isothermes de l'acide carbonique. Comptes Rendus Hebdomadaires des Séances de l'Académie des Sciences, 113, 446–451.

Angus, S., Armstrong, B., and de Reuck, K.M. (1973) International thermodynamic tables of the fluid state, vol. 3: Carbon dioxide. Pergamon Press, Oxford.

Baker, E.H. (1962) The calcium oxide–carbon dioxide system in the pressure range 1–300 atmospheres. Journal of the Chemical Society, 464–470.

Bell, P.M., and England, J.L. (1964) High pressure differential thermal analysis of a fast reaction with $CaCO_3$. Carnegie Institution of Washington Year Book, 63, 176–178.

Berman, R.G. (1988) Internally-consistent thermodynamic data for minerals in the system Na_2O-K_2O-CaO-MgO-FeO-Fe_2O_3-Al_2O_3-SiO_2-TiO_2-H_2O-CO_2. Journal of Petrology, 29, 445–522.

Berman, R.G., and Brown, T.H. (1985) The heat capacity of minerals in the system K_2O-Na_2O-CaO-MgO-FeO-Fe_2O_3-Al_2O_3-SiO_2-TiO_2-H_2O-CO_2: Representation, estimation, and high temperature extrapolation. Contributions to Mineralogy and Petrology, 89, 168–183.

Berman, R.G., Engi, M., Greenwood, H.J., and Brown, T.H. (1986) Derivation of internally-consistent thermodynamic data by the technique of mathematical programming: A review with application to the system MgO-SiO_2-H_2O. Journal of Petrology, 27, 1331–1364.

Boeke, H.E. (1912) Die Schmelzerscheinungen und die umkehrbare Umwandlung des Calciumcarbonats. Neues Jahrbuch der Mineralogie und Geologie, 1, 91–121.

Boettcher, A.L., and Wyllie, P.J. (1968) The calcite-aragonite transition measured in the system CaO-CO_2-H_2O. Journal of Geology, 76, 324–330.

Bottinga, Y., and Richet, P. (1981) High pressure and temperature equation of state and calculation of thermodynamic properties of gaseous carbon dioxide. American Journal of Science, 218, 615–660.

Brown, T.H., Berman, R.G., and Perkins, E.H. (1988) Ge0-Calc: Software package for calculation and display of pressure-temperature-composition phase diagrams using an IBM or compatible personal computer. Computers and Geoscience, 14, 279–289.

Chernosky, J.V., and Berman, R.G. (1989) Experimental reversal of the equilibrium: Clinochlore + 2 magnesite = 3 forsterite + spinel + 2 CO_2 + 4 H_2O and revised thermodynamic properties for magnesite. American Journal of Science, 289, 249–266.

Clark, S.P., Jr. (1957) A note on calcite-aragonite equilibrium. American Mineralogist, 42, 564–566.

Cohen, L.C., and Klement, W. (1973) Determination of high temperature transition in calcite to 5 kbar by differential thermal analysis in hydrostatic apparatus. Journal of Geology, 81, 724–726.

Crawford, W.A., and Fyfe, W.S. (1964) Calcite-aragonite equilibrium at 100 °C. Science, 144, 1569–1570.

Crawford, W.A., and Hoersch, A.L. (1972) Calcite-aragonite equilibrium from 50 °C to 150 °C. American Mineralogist, 57, 985–998.

de Santis, R., Breedveld, G.J.F., and Prausnitz, J.M. (1974) Thermodynamic properties of aqueous gas mixtures at advanced pressures. Industrial Engineering Chemistry Process Design and Development, 13, 374–377.

Dove, M.T., and Powell, B.M. (1989) Neutron diffraction study of the tricritical orientational order/disorder phase transition in calcite at 1260 K. Physics and Chemistry of Minerals, 16, 503–507.

Eggler, D.H., Kushiro, I., and Holloway, J.R. (1979) Free energy of decarbonation reactions at mantle pressures: I. Stability of the assemblage forsterite-enstatite-magnesite in the system MgO-SiO_2-CO_2-H_2O to 60 kbar. American Mineralogist, 64, 288–293.

Eitel, W. (1923) Über das binäre System $CaCO_3$-Ca_2SiO_4 und den Spurrit. Neues Jahrbuch der Mineralogie, Geologie und Paläontologie, Beilageband, 48, 63–74.

Ferry, J.M., and Baumgartner, L. (1987) Thermodynamic models of molecular fluids at the elevated pressures and temperatures of crustal metamorphism. In Mineralogical Society of America Reviews in Mineralogy, 17, 323–365.

Getting, I.C., and Kennedy, G.C. (1970) Effect of pressure on the emf of chromel-alumel and platinum-platinum 10% rhodium thermocouples. Journal of Applied Physics, 41, 4552–4562.

Goldsmith, J.R., and Heard, H.C. (1961) Subsolidus phase relations in the system $CaCO_3$-$MgCO_3$. Journal of Geology, 69, 45–74.

Greenwood, H.J. (1967) Mineral equilibria in the system MgO-SiO_2-H_2O-CO_2. In P.H. Abelson, Ed., Researches in geochemistry, vol. 2, p. 542–567. Wiley, New York.

Harker, R.I., and Tuttle, O.F. (1955) Studies in the system CaO-MgO-CO_2. Part I: The thermal dissociation of calcite, dolomite, and magnesite. American Journal of Science, 253, 209–224.

——— (1956) Experimental data on the P_{CO_2}-T curve for the reaction: calcite + quartz = wollastonite + carbon dioxide. American Journal of Science, 254, 239–256.

Haselton, H.T., Jr., Sharp, W.E., and Newton, R.C. (1978) CO_2 fugacity at high temperatures and pressures from experimental decarbonation reactions. Geophysical Research Letters, 5, 753–756.

Helffrich, G.R., and Wood, B.J. (1989) High pressure fluid *P-V-T* properties from fluid perturbation theory. Eos, 70, 487.

Holland, T.J.B., and Powell, R. (1990) An enlarged and updated internally consistent thermodynamic dataset with uncertainties and correlations: The system K_2O-Na_2O-CaO-MgO-MnO-FeO-Fe_2O_3-Al_2O_3-TiO_2-SiO_2-C-H_2-O_2. Journal of Metamorphic Geology, 8, 89–124.

Holloway, J.R. (1977) Fugacity and activity of molecular species in supercritical fluids. In D.G. Fraser, Ed., Thermodynamics in geology, p. 161–181. Reidel, Dodrecht, Holland.

——— (1981a) Volatile melt interactions. In R.C. Newton, A. Navrotsky, and B.J. Wood, Eds., Advances in physical geochemistry, vol. 1, p. 266–286. Springer-Verlag, New York.

——— (1981b) Compositions and volumes of supercritical fluids in the earth's crust. In L.S. Hollister and M.L. Crawford, Eds., Short course in fluid inclusions: Applications to petrology, vol. 6, p. 13–35. Mineralogical Association of Canada, Toronto.

——— (1987) Igneous fluids. In Mineralogical Society of America Reviews in Mineralogy, 17, 211–233.

Huang, W., and Wyllie, P.J. (1975) Melting reactions in the system $NaAlSi_3O_8$-$KAlSi_3O_8$-SiO_2 to 35 kilobars, dry and with excess water. Journal of Geology, 83, 737–748.

Irving, A.J., and Wyllie, P.J. (1975) Subsolidus and melting relationships for calcite, magnesite, and the join $CaCO_3$-$MgCO_3$ to 36 kb. Geochimica et Cosmochimica Acta, 39, 35–53.

Jacobs, G.K., Kerrick, D.M., and Krupka, K.M. (1981) The high temperature heat capacity of natural calcite ($CaCO_3$). Physics and Chemistry of Minerals, 7, 55–59.

Johannes, W. (1969) An experimental investigation of the system MgO-SiO_2-H_2O-CO_2. American Journal of Science, 267, 1083–1104.

Johannes, W., and Metz, P. (1968) Experimentelle Bestimmung von Gleichgewichtsbeziehungen im System MgO-CO_2-H_2O. Neues Jahrbuch der Mineralogie Monatshefte, 112, 15–26.

Johannes, W., and Puhan, D. (1971) The calcite-aragonite transition reinvestigated. Contributions to Mineralogy and Petrology, 31, 28–38.

Juza, J. (1961) An equation of state for water and steam, and steam tables in the critical region and in the range from 1000 to 100000 bars. Rada Technickyeh VED, Prag, 76, 3–121.

Juza, J., Kmoníček, V., and Šifner, O. (1965) Measurement of the specific volume of carbon dioxide in the range of 700 to 4000 b and 50 to 475 °C. Physica, 31, 1735–1744.

Kelly, K.K. (1960) Contributions to the data on theoretical metallurgy. XIII. High temperature heat-content, heat-capacity, and entropy data for the elements and inorganic compounds. U.S. Bureau of Mines Bulletin, 584, 232 p.

Kennedy, G.C. (1954) Pressure-volume-temperature relations in CO_2 at elevated temperatures and pressures. American Journal of Science, 252, 225–241.

Kerrick, D.M., and Jacobs, C.K. (1981) A modified Redlich-Kwong equation for H_2O, CO_2, and H_2O-CO_2 mixtures at elevated pressures and temperatures. American Journal of Science, 281, 735–767.

Kobayashi, K. (1950a) The heat capacity of inorganic substances at high temperatures, part III. The heat capacity of synthetic calcite (calcium carbonate). Science Reports, University of Tokyo, 34, 103–110.

——— (1950b) The heat capacity of inorganic substances at high temperatures, part IV. The heat capacity of synthetic aragonite (calcium carbonate). Science Reports, University of Tokyo, 34, 111–118.

Kozu, S., and Kani, K. (1934) Thermal expansion of aragonite and its atomic displacements by transformation into calcite between 450 °C and 490 °C in air, I. Proceedings of the Imperial Academy of Japan, 10, 222–225.

Lander, J.J. (1949) Polymorphism and anion rotational disorder in the alkaline earth carbonates. Journal of Chemical Physics, 17, 892–901.

Lasden, L.S., and Waren, A.D. (1982) GRG2 user's guide. Cleveland State University, Cleveland, Ohio.

Madelung, E., and Fuchs, R. (1921) Kompressibiltätsmessungen an festen Körpern. Annalen der Physik, 65, 289–309.

Mäder, U.K. (1990) Carbon dioxide and carbon dioxide-water mixtures: P-V-T properties and fugacities to high pressure and temperature constrained by thermodynamic analysis and phase equilibrium experiments, 180 p. Unpublished Ph.D. thesis, The University of British Columbia, Vancouver, British Columbia.

Mäder, U.K., Berman, R.G., and Greenwood, H.J. (1988) An equation of state for carbon dioxide consistent with phase equilibrium data: 400–2000 K, 1 bar–50 kbar. Geological Society of America Abstracts with Programs, 20, A190.

Markgraf, S.A., and Reeder, R.J. (1985) High-temperature structure refinements of calcite and magnesite. American Mineralogist, 70, 590–600.

Mel'nik, Y.P. (1972) Thermodynamic parameters of compressed gases and metamorphic reactions involving water and carbon dioxide. Geochemistry International, 9, 419–426 (translated from Geokhimiya, no. 6, 654–662, 1972).

Michels, A., and Michels, C. (1935) Isotherms of CO_2 between 0° and 150° and pressures from 16 to 250 atmospheres. Proceedings of the Royal Society of London, Series A, 153, 201–214.

Michels, A., Michels, C., and Wouters, H.H. (1935) Isotherms of CO_2 between 70 and 3000 atmospheres. Proceedings of the Royal Society of London, Series A, 153, 214–224.

Mirwald, P.W. (1976) A differential thermal analysis study of the high-temperature polymorphism of calcite at high pressure. Contributions to Mineralogy and Petrology, 59, 33–40.

——— (1979a) Determination of a high-temperature transition of calcite at 800 °C and one bar CO_2 pressure. Neues Jahrbuch der Mineralogie Monatshefte, 7, 309–315.

——— (1979b) The electrical conductivity of calcite between 300 and 1200 °C at a CO_2 pressure of 40 bars. Physics and Chemistry of Minerals, 4, 291–297.

Mirwald, P.W., Getting, I.C., and Kennedy, G.C. (1975) Low-friction cell for piston-cylinder high-pressure apparatus. Journal of Geophysical Research, 80, 1519–1525.

Newton, R.C., and Sharp, W.C. (1975) Stability of forsterite + CO_2 and its bearing on the role of CO_2 in the mantle. Earth and Planetary Science Letters, 26, 239–244.

Philipp, R. (1988) Phasenbeziehungen im System MgO-H_2O-CO_2-$NaCl$. Unpublished Ph.D. thesis, ETH Zurich, no. 8641.

Powell, R., and Holland, T.J.B. (1985) An internally consistent thermodynamic dataset with uncertainties and correlations: 1. Methods and a worked example. Journal of Metamorphic Geology, 3, 327–342.

Prausnitz, J.M., Lichtenthaler, R.N., and de Azevedo, E.G. (1986) Molecular thermodynamics of fluid-phase equilibria (2nd edition), 600 p. Prentice-Hall, Englewood Cliffs, New Jersey.

Redlich, O., and Kwong, J.N.S. (1949) On the thermodynamics of solutions. V. An equation of state. Fugacities of gaseous solutions. Chemical Reviews, 44, 233–244.

Robie, R., Hemingway, B.S., and Fisher, J.R. (1979) Thermodynamic properties of minerals and related substances at 298.15 K and 1 bar (10^5 Pascals) pressure and higher temperatures. U.S. Geological Survey Bulletin, 1452, 456 p.

Ross, M., and Ree, F.H. (1980) Repulsive forces of simple molecules and mixtures at high density and temperature. Journal of Chemical Physics, 73, 6146–6152.

Ryzhenko, B.N., and Volkov, V.P. (1971) Fugacity coefficients of some gases in a broad range of temperatures and pressures. Geochemistry International, 8, 468–481 (translated from Geokhimiya, no. 7, 760–773, 1971).

Salje, E., and Viswanathan, K. (1976) The phase diagram calcite-aragonite as derived from the crystallographic properties. Contributions to Mineralogy and Petrology, 55, 55–67.

Saxena, S.K., and Fei, Y. (1987a) High pressure and high temperature fluid fugacities. Geochimica et Cosmochimica Acta, 51, 783–791.

——— (1987b) Fluids at crustal pressures and temperatures, I. Pure species. Contributions to Mineralogy and Petrology, 95, 370–375.

Shmonov, V.M., and Shmulovich, K.I. (1974) Molar volumes and equation of state of CO_2 at temperatures from 100–1000 °C and pressures from 2000–10000 bars. Doklady Akademiia Nauk SSSR, 217, 935–938 (in Russian).

Shmulovich, K.I. (1974) Phase equilibria in the system CaO-Al_2O_3-SiO_2-CO_2. Geochemistry International, 11, 883–887.

Shmulovich, K.I., and Shmonov, V.M. (1975) Fugacity coefficients for CO_2 from 1.0132 to 10000 bar and 450–1300 K. Geochemistry International, 12, 202–206 (translated from Geokhimiya, no. 9, 551–555, 1975).

Singh, A.K., and Kennedy, G.C. (1974) Compression of calcite to 40 kbar. Journal of Geophysical Research, 79, 2615–2622.

Smith, F.H., and Adams, L.H. (1923) The system calcium oxide–carbon dioxide. Journal of the American Chemical Society, 45, 1167–1184.

Stavely, L.A.K., and Linford, R.G. (1969) The heat capacity and entropy of calcite and aragonite, and their interpretation. Journal of Chemical Thermodynamics, 1, 1–11.

Touret, J., and Bottinga, Y. (1979) Équation d'état pour le CO_2; Application aux inclusions carboniques. Bulletin Minéralogique, 102, 577–583.

Treiman, A.H., and Essene, E.J. (1983) Phase equilibria in the system CaO-SiO_2-CO_2. American Journal of Science, 283-A, 97–120.

Trommsdorff, V., and Connolly, J.A.D. (1990) Constraints on phase diagram topology for the system CaO-MgO-SiO_2-CO_2-H_2O. Contributions to Mineralogy and Petrology, 104, 1–7.

Tsiklis, D.S., Linshits, L.R., and Tsimmerman, S.S. (1971) Measurement and calculation of molar volumes of carbon dioxide at high pressure and temperature. Teplofizicheskie Svoistva Veshchestv İ Materialov, 3, 130–136 (in Russian).

Vukalovich, M.P., Altunin, V.V., and Timoshenko, N.I. (1962) Experimental investigation of the specific volume of carbon dioxide at temperatures from 200–750 °C and pressures up to 600 kg/cm². Teploenergetica, 9, 56–62 (in Russian).

——— (1963a) Experimental determination of the specific volume of CO_2 at temperatures 40–150 °C and pressures up to 600 kg/cm². Teploenergetica, 10, 85–88 (in Russian).

——— (1963b) Specific volume of carbon dioxide at high pressure and temperature. Teploenergetica, 10, 92–93 (in Russian).

Walter, L.S. (1963a) Experimental studies on Bowen's decarbonation series: I: P-T univariant equilibria of the 'monticellite' and 'akermanite' reactions. American Journal of Science, 261, 488–500.

——— (1963b) Experimental studies on Bowen's decarbonation series: II: P-T univariant equilibria of the reaction: forsterite + calcite = monticellite + periclase + CO_2. American Journal of Science, 261, 773–779.

Wasil, E., Golden, B., and Liu, L. (1989) State-of-the-art in nonlinear optimization software for the microcomputer. Computers and Operations Research, 16, 497–512.

Zubarev, V.N., and Telegin, G.S. (1962) The impact compressibility of liquid nitrogen and solid carbon dioxide. Soviet Physics, Doklady, 7, 34–36.

MANUSCRIPT RECEIVED SEPTEMBER 24, 1990
MANUSCRIPT ACCEPTED MAY 14, 1991

APPENDIX 1. INTEGRATION OF THE EQUATION OF STATE

The quantity $\int_{P_0}^{P} V_{CO_2}^{T}\,dP$ is most easily obtained from the relationship

$$\int_{P_0}^{P} V\,dP$$

$$= \int_{V_P}^{V_0} P\,dV + V_P(P - P_0) - P_0(V_0 - V_P)$$

$$= \int_{V_P}^{V_0} \frac{RT}{V - \left(B - \dfrac{B_3}{V^3 - C}\right)}\,dV$$

$$- \int_{V_P}^{V_0} \frac{A_1}{TV^2}\,dV + \int_{V_P}^{V_0} \frac{A_2}{V^4}\,dV$$

$$+ V_P(P - P_0) - P_0(V_0 - V_P) \qquad \text{(A1)}$$

with $B = B_1 + B_2T$ and $C = B_3/B$.

The attractive terms (A_1 and A_2 terms) become upon integration

$$\frac{A_1}{T}\left(\frac{1}{V_0} - \frac{1}{V_P}\right) - \frac{A_2}{3}\left(\frac{1}{V_0^3} - \frac{1}{V_P^3}\right). \qquad \text{(A2)}$$

The repulsive term (RT term) requires integration of a rational function of the form

$$\int_{V_P}^{V_0} \frac{mV^3 + n}{V(aV^3 + bV^2 + cV + d)}\,\mathrm{d}V \qquad \text{(A3)}$$

with $m = \mathrm{R}T$, $n = \mathrm{R}T\mathrm{C}$, $a = 1$, $b = -\mathrm{B}$, $c = 0$, $d = \mathrm{C} = B_3/B$, and $B = B_1 + B_2T$.

Integral A3 may be solved after splitting into partial fractions provided the real roots of the polynomial $aV^3 + bV^2 + cV + d$ are known.

Case 1. Polynomial $aV^3 + bV^2 + cV + d$ yields three real roots X_1, X_2, X_3. Integral A3 may be split into partial fractions by solving

$$\frac{mV^3 + n}{V(aV^3 + bV^2 + cV + d)} = \frac{I}{V} + \frac{J}{V - X_1} + \frac{K}{V - X_2} + \frac{L}{V - X_3}. \qquad \text{(A4)}$$

Cross multiplication and collecting terms in powers of V yield four equations in four unknowns (I, J, K, L) by comparing coefficients:

$$n = I(-X_1X_2X_3) \qquad \text{(A5)}$$

$$0 = I(X_1X_2 + X_1X_3 + X_2X_3) + J(X_2X_3) + K(X_1X_3) + L(X_1X_2) \qquad \text{(A6)}$$

$$0 = I(X_1 + X_2 + X_3) + J(X_2 + X_3) + K(X_1 + X_3) + L(X_1 + X_2) \qquad \text{(A7)}$$

$$m = I + J + K + L. \qquad \text{(A8)}$$

Equations A5 through A8 are solved simultaneously to obtain

$$I = -\frac{n}{X_1X_2X_3} \qquad \text{(A9)}$$

$$J = -\frac{mX_1^3 + n}{X_1(-X_1^2 + X_1X_2 - X_2X_3 + X_1X_3)} \qquad \text{(A10)}$$

$$K = \frac{mX_2^3 + n}{X_2(X_2^2 - X_1X_2 - X_2X_3 + X_1X_3)} \qquad \text{(A11)}$$

$$L = \frac{mX_3^3 + n}{X_3(X_3^2 + X_1X_2 - X_2X_3 - X_1X_3)}. \qquad \text{(A12)}$$

Integral A3 may now be integrated by parts to obtain

$$I \ln\left(\frac{V_0}{V_P}\right) + J \ln\left(\frac{V_0 - X_1}{V_P - X_1}\right) + K \ln\left(\frac{V_0 - X_2}{V_P - X_2}\right) + L \ln\left(\frac{V_0 - X_3}{V_P - X_3}\right). \qquad \text{(A13)}$$

Case 2. Polynomial $aV^3 + bV^2 + cV + d$ yields one real root X_1. Integral A3 may be split into partial fractions by solving

$$\frac{mV^3 + n}{V(aV^3 + bV^2 + cV + d)} = \frac{I}{V} + \frac{J}{V - X_1} + \frac{KV + L}{V^2 + \alpha V + \beta} \qquad \text{(A14)}$$

with $\alpha = b/a + X_1$ and $\beta = c/a + X_1\alpha$, which yields four equations in four unknowns (I, J, K, L):

$$n = -I\beta X_1 \qquad \text{(A15)}$$

$$0 = I(\beta - \alpha X_1) + J\beta - LX_1 \qquad \text{(A16)}$$

$$0 = I(\alpha - X_1) + J\alpha - KX_1 + L \qquad \text{(A17)}$$

$$m = I + J + K. \qquad \text{(A18)}$$

Equations A15 through A18 are solved simultaneously to obtain

$$I = -\frac{n}{\beta X_1} \qquad \text{(A19)}$$

$$J = -\frac{mX_1^3 + n}{X_1(\alpha X_1 + \beta + X_1^2)} \qquad \text{(A20)}$$

$$K = \frac{\alpha\beta m X_1 + \alpha n + \beta^2 m + nX_1}{\beta(\alpha X_1 + \beta + X_1^2)} \qquad \text{(A21)}$$

$$L = \frac{\alpha^2 n + \alpha n X_1 + \beta^2 m X_1 - \beta n}{\beta(\alpha X_1 + \beta + X_1^2)}. \qquad \text{(A22)}$$

The last term of Equation A14 is expanded to standard integrals by appropriate substitutions:

$$\int \frac{KV + L}{V^2 + \alpha V + \beta}\,\mathrm{d}V = \int \frac{Kz}{z^2 + t^2}\,\mathrm{d}z + \int \frac{L - Ks}{z^2 + t^2}\,\mathrm{d}z \qquad \text{(A23)}$$

with $z = V + s$, $s = \alpha/2$, $t = \sqrt{\beta - s^2}$, and $\mathrm{d}V = \mathrm{d}z$.

Integration of A3 yields

$$I \ln\left(\frac{V_0}{V_P}\right) + J \ln\left(\frac{V_0 - X_1}{V_P - X_1}\right) + \frac{K}{2} \ln\left(\frac{(V_0 + s)^2 + t^2}{(V_P + s)^2 + t^2}\right) + \frac{L - Ks}{t}\left[\arctan\left(\frac{V_0 + s}{t}\right) - \arctan\left(\frac{V_P + s}{t}\right)\right] \qquad \text{(A24)}$$

with $\alpha = b/a + X_1$, $\beta = c/a + \alpha X_1$, $s = \alpha/2$, and $t = \sqrt{\beta - s^2}$.